Morphology of Crosslinked Hyaluronic Acid Porous Hydrogels

Maurice N. Collins,[1] Colin Birkinshaw[2]

[1]*Stokes Research Institute, University of Limerick, Limerick, Ireland*
[2]*Department of Materials Science and Technology, University of Limerick, Limerick, Ireland*

Received 25 March 2010; accepted 20 August 2010
DOI 10.1002/app.33241
Published online 8 November 2010 in Wiley Online Library (wileyonlinelibrary.com).

ABSTRACT: Hydrogels, based on hyaluronic acid or hyaluronan (HA), are gaining attention as possible cell-scaffolding materials for the regeneration of a variety of tissues. This article describes how HA, a naturally occurring polymer, has been crosslinked to reduce its degradation rate and freeze dried to produce porous materials suitable for tissue engineering. The resulting pore architecture has been assessed as a function of freezing temperature and freezing rate, type of crosslinkers, and methods used in the crosslinking process. On comparing the average densities of crosslinked and uncrosslinked scaffolds, it is apparent that the chemical modification increases sponge density and wall thickness of the pores while decreasing the pore size. The mechanical response of the modified materials has been investigated by equilibrium-swelling measurements and compression tests. These materials have an average pore size ranging from 167 to 215 μm, which suggests that they would be a suitable temporary site for cell proliferation. The materials exhibit moderate mechanical integrity and are expected to be capable of withstanding physiological stresses *in vivo*. © 2010 Wiley Periodicals, Inc. J Appl Polym Sci 120: 1040–1049, 2011

Key words: biomaterials; hydrogels; morphology; crosslinking

INTRODUCTION

Tissue engineering has emerged as a potentially effective approach to the repair and/or replacement of damaged or diseased tissue.[1–8] The challenge is to design a scaffold that provides the newly regenerating tissue with a temporary site for cell attachment, proliferation, and mechanical stability. This is achieved by seeding the cells onto porous matrices, known as scaffolds, to which the cells attach and proliferate. This scaffold should also be capable of withstanding the normal physiological stress found at the implant site while providing a platform for the growth of cells into the required three-dimensional organ or tissue.

Such a scaffold should be biocompatible and resorbable[9–14] and should not elicit a permanent foreign body reaction and be eventually reabsorbed and replaced by natural tissue. Porosity also plays an important role in the function of the implant as mass transport of nutrients and must be possible to facilitate seeding and subsequent cell proliferation. Important parameters are pore size and size distribution, pore interconnection size, total pore surface area, and morphology.

Correspondence to: M. N. Collins (maurice.collins@ul.ie).

Journal of Applied Polymer Science, Vol. 120, 1040–1049 (2011)

Hydrogel-scaffolding materials have many different functions in the field of tissue engineering. As a filling material, they are used to treat conditions such as urinary incontinence[15] and have potential roles in both plastic and reconstructive surgery.[16] A scaffold allowing for local and specific drug targeting to the desired tissue site is highly desirable in many situations as it reduces the need for large doses.[3] Varieties of other hydrogel systems have been previously used or are in development for bioactive molecule delivery; for example, the angiogenesis promoting growth factor and VEGF has been incorporated into ionically crosslinked alginate hydrogels[17] and in glutaraldehyde (GTA) crosslinked collagen sponges by Tabata.[18] Collagen,[19] chitosan-gelatin,[20] polyethylene glycol,[21] and hyaluronic acid (HA)[3] have all proved useful as scaffolds for soft tissue-engineering applications.

The easy development of highly porous networks is a necessity when considering any material as a potential scaffolding matrix in tissue engineering to facilitate cell seeding and ingrowth. The pore size must be within a critical range of 20–200 μm, depending upon application, so that the cells are housed in a compartment with sufficient space to grow and attach well to the material. Porous networks extending through an implant increases the surface area, allowing a greater number of cells to attach to the matrix. This enhances the regenerative properties of the implant by allowing the tissue ingrowth directly onto the interior of the matrix.

Hutmacher[22] has identified the following requirements for tissue engineering scaffolds (a) the scaffold should possess interconnecting pores of appropriate scale to favor tissue integration and vascularization, (b) be made from material with controlled biodegradability or bioresorbability, so that tissue will eventually replace the scaffold, (c) have appropriate surface chemistry to favor cellular attachment, differentiation, and proliferation, (d) possess adequate mechanical properties to match the intended site of implantation and handling, (e) should not induce any adverse response, and (f) be easily fabricated into a variety of shapes and sizes.

The fabrication of scaffolds from HA a natural resorbable material can impart intrinsic signals[23,24] within the structure that can enhance tissue formation. HA is a glycosaminoglycan copolymer of D-glucuronic acid and *N*-acetyl-D-glucosamine and is a major intracellular component (IC) of connective tissues. HA plays an important role in lubrication, cell differentiation, and cell growth. Cellular interactions with HA can occur through cell-surface receptors (CD44,[25,26] RHAMM,[23] and ICAM-1[27]) and influence processes such as wound repair, inflammation, and metastasis.[28] HA in solution has been used in clinical applications including ocular surgery,[29] viscosupplementation for arthritis,[30,31] and the prevention of postoperative adhesion between two healing tissue surfaces.[32,33] However, the poor mechanical properties, rapid hydrolytic degradation, and *in vivo* clearance of uncrosslinked soluble HA limit many direct clinical applications. However, previous studies have shown that, when crosslinked, its rate of hydrolytic degradation can be controlled,[34,35] it will possess adequate mechanical stability, and it can be easily fabricated into a variety of shapes.[36]

In this article, the fabrication of porous resorbable hydrogel scaffolds from HA using a freeze drying process is described. These scaffolds have the potential to be used in low load-bearing applications such as soft tissue repair and wound healing. The resulting scaffolds possess interconnecting pores of appropriate size suitable for hosting cells and tissue regeneration. The effects of process variables such as freezing rate and temperature on the pore size and distribution are assessed. A minimum pore size of 150 μm has been suggested in the literature for bone[37] and 200–250 μm for soft tissue.[38] Therefore, the objective of this work was to produce degradable scaffolds with a target overall porosity between 90 and 95%, consisting of pores with an average diameter between 100 and 300 μm. Scaffold morphology has been assessed by scanning electron morphology and statistical analysis of pore size distribution obtained through optical microscopy. Swelling ratio (SR) in water has also been assessed along with mechanical compression measurement.

EXPERIMENTAL

Materials

HA with a molecular weight of 2 million Daltons was supplied by Clear Solutions (USA) in powdered form. 1-Ethyl-3-(3-dimethylaminopropyl) carbodiimide (EDC), GTA, poly(ethylene glycol) diglycidyl ether, and divinyl sulfone (DVS) were purchased from Lancaster, UK. Solutions were prepared by sieving HA particles into double-distilled water to expose the maximum area for solvent interaction. This was followed by agitation to minimize shear stress in a shaking bath at 25°C for up to 102 h and found to give reproducible solutions of uniform viscosity. Samples were fully dissolved after 24 h.

Scaffold preparation

The chemistry and methodology of HA crosslinking, using both homogenous and heterogenous systems, has been described in detail previously,[34,35] Homogeneous crosslinking involves incorporation of the crosslinking agent directly into the HA solution, whereas heterogeneous methods rely upon immersing a HA sponge in a solution of the crosslinking agent. Following the procedures referred to, powdered HA with a molecular weight of 2 million Daltons was dissolved in distilled water (in 0.2*M* NaOH for DVS crosslinked samples) by agitation for 24 h to give solutions of 1 and 4 wt % concentration. Once dissolved, the pH of each solution was adjusted to suit the crosslinker used. Homogeneous crosslinking was carried out by inclusion of the crosslinking agent into the HA solution, whereas heterogeneous crosslinking was carried out using HA scaffolds, which were immersed in crosslinker solution containing a 10-mL acetone-water (80 : 20 by volume) with adjusted pH levels depending on the crosslinker being used.

HA solutions were then poured into 35-mm polystyrene petri dishes to a depth of $\sim$ 5 mm or into 12.7-mm diameter plastic vials to a final volume of 7 mL. Crosslinking reagents included GTA, ethylene glycol diglycidyl ether (EX 810), 1-EDC) with L-leucine methyl ester (LME), and DVS. Although full details of the chemistry of these crosslinkers have been given,[34,35] it should be noted that the effectiveness of the crosslinkers can be ranked based on their stability while immersed in distilled water as follows GTA, DVS, EDC (performance improved with LME addition), and EX 810.

The process of "autocrosslinking" by simply solution freezing has been reported.[39] The presumption is that, at sufficiently low temperatures, the semipermanent chain entanglements and secondary bond associations are established and that these persist when the solution is thawed out giving gel character to the solution.

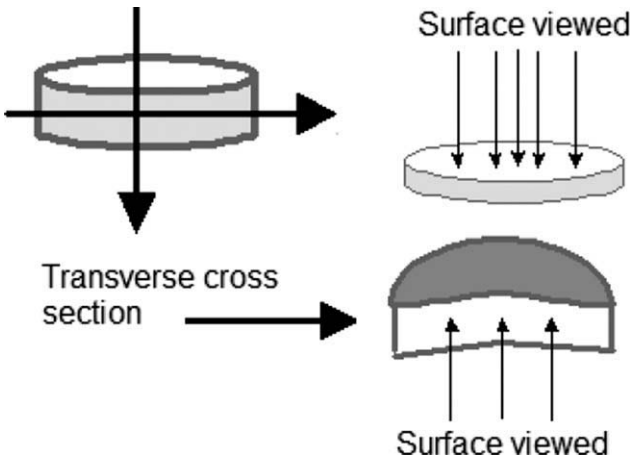

Figure 1 Graphical representation of the sections for SEM.

Solutions were placed in cylindrical containers to produce samples as shown in Figure 1. The solutions were then placed into the chamber of a freeze-dryer (VirTis, Advantage) at 20°C. The thickness of the scaffolds could be varied by varying the quantity of solution within the molds. The temperature of the freeze-dryer shelf and chamber was cooled at a constant rate to the final temperature of freezing (T_f); the shelf/chamber temperature was then held constant for 60 min at T_f to complete the freezing process. Final temperatures of freezing of −10°C, −20°C, −30°C, and −40°C were used to produce porous scaffolds of four different mean pore sizes. The ice phase was then sublimated under vacuum (<100 mTorr) for a period of 17 h to produce the interconnecting, porous structure of the scaffolds. To evaluate the time needed to freeze HA solutions, a thermocouple was inserted into one of the solutions in a 35-mm petri dish during the freezing process. To improve the mechanical performance of the scaffolds, they were immersed in crosslinker solutions similar to the method used in film crosslinking.[34]

Analysis of pore structure

Sponges prepared from varying concentrations of HA were examined with scanning electron microscopy (SEM) to observe their morphological features. The samples were initially coated with gold with an Edwards Sputter Coater SI50B. SEM photomicrographs were obtained by a JEOL JSM-840 scanning electron microscope for each of the disk sponges in both planar and transverse cross sections (see Fig. 1). Sections were obtained by cutting the sponge samples with a thin blade and were sputter-coated with gold using an Edwards Sputter Coater SI50B to make them conductive. Each of these samples was cut from the top surface through the entire depth of the scaffold (~ 5 mm).

SEM images were analyzed and evaluated for surface pore size and the appearance of an interconnecting pore structure, pore fraction, and average pore diameter. Although every attempt was made to

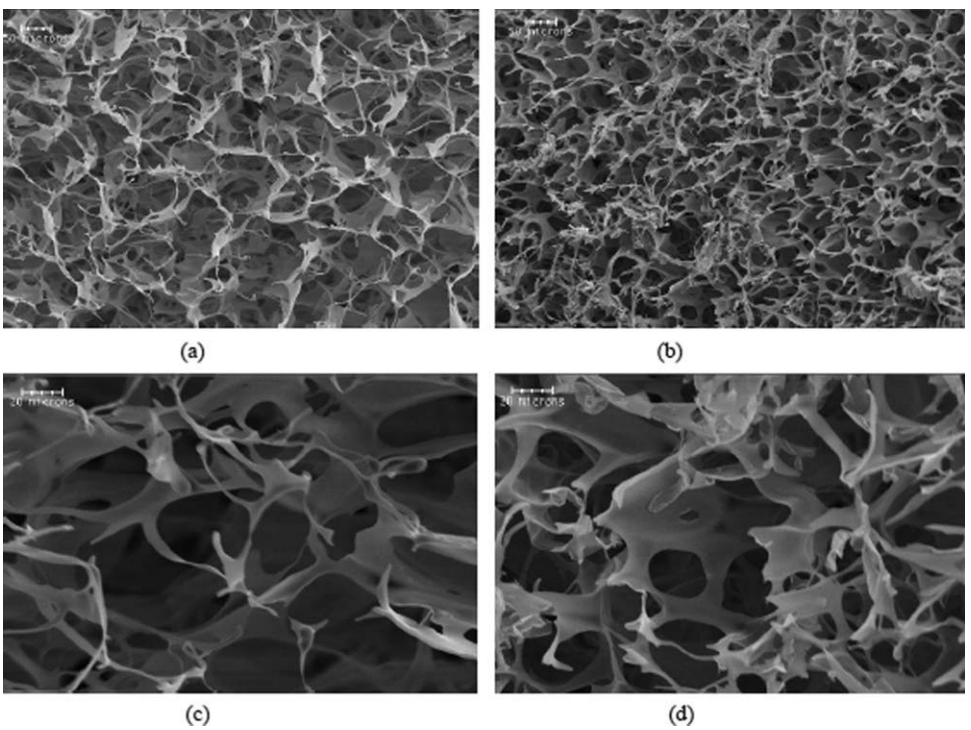

Figure 2 (a) 1% solution (150× magnification), (b) 4% solution (150× magnification), (c) 1% solution (500× magnification), and (d) 4% solution (500× magnification).

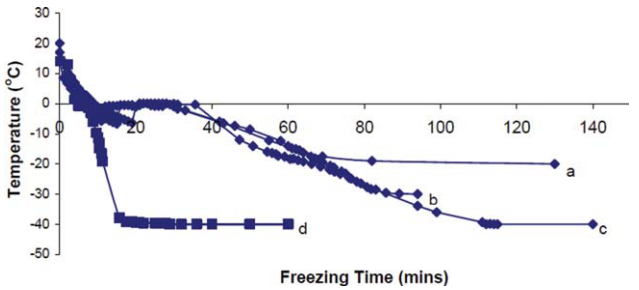

Figure 3 Freezing profile of the hyaluronic acid solution in the freeze dryer with the temperature monitored by a thermocouple within the solution. The freezing rate for a, b, and c was 0.6°C/min and 3.4°C/min for d. [Color figure can be viewed in the online issue, which is available at wileyonlinelibrary.com.]

keep magnifications consistent throughout all samples, deviations from the set values were necessary with some samples to improve resolution and focus.

Sponge density was obtained by dimensional measurement and weighing

The images obtained through SEM processing were further analyzed with Enterprise (BEUHLER) software to determine the average pore size and wall thickness of the pores of the various sponges produced by the freeze-drying process.

Water uptake properties of scaffolds

SR was calculated via the equation:

$$\text{Swelling ratio} = \frac{W_s}{W_d} \tag{1}$$

where W_s is the weight of the sample at equilibrium at each temperature and W_d is the weight of the dried sample and the equilibrium water content (EWC) defined by,

$$\text{EWC} = \frac{(\text{SR} - 1)}{\text{SR}} \tag{2}$$

Prepared gels were immersed in either distilled water or phosphate-buffered saline solution for various periods of time at 25°C and 37°C. The swollen gel was then carefully taken out from the solution, wiped with a filter paper to remove free water on the surface, and then weighed. All measurements were made in triplicate.

Mechanical testing of scaffolds

Crosslinked scaffolds were compression tested using a compression rig on an Instron 4302 universal tester. A load cell of 100 N was used with a crosshead speed of 1.25 mm/min. The shape of a typical sample tested under compression is shown in Figure 1.

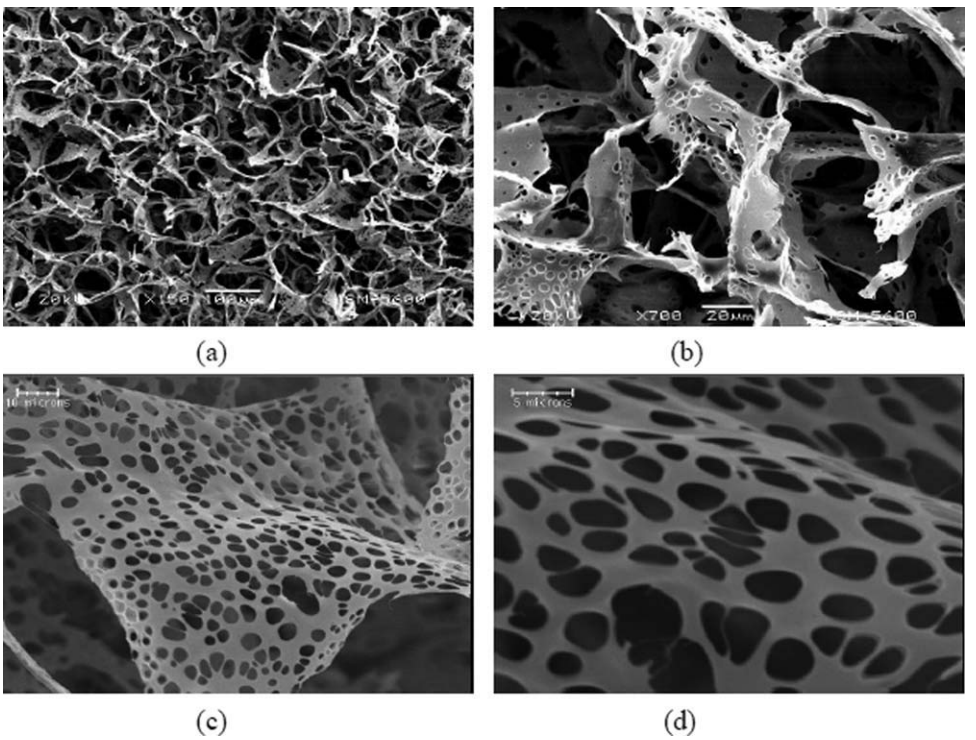

Figure 4 (a) Uncrosslinked porous scaffold produced from a freezing rate of 3.4°C/min (150× magnification); (b) (700× magnification); (c) layer of HA within the uncrosslinked scaffold (1000× magnification); and (d) (3000× magnification). Average pore size of the layer was 6 μm.

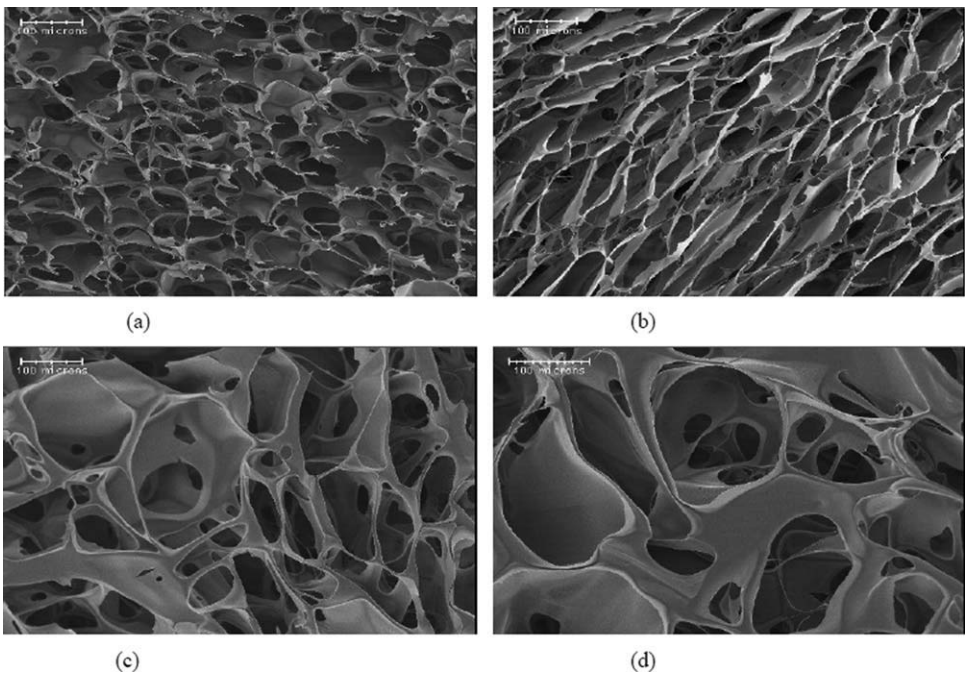

Figure 5 (a) Transverse section of HA frozen at −10°C (150× magnification), (b) planar cross section of HA frozen at −10°C (150× magnification), (c) transverse section of HA frozen at −20°C (150× magnification), and (d) planar cross section of HA frozen at −20°C (200× magnification).

RESULTS AND DISCUSSION

To establish a HA concentration that would produce structurally stable porous scaffolds, 1 and 4 wt % HA solutions were prepared as outlined earlier. The solutions were degassed under a vacuum and frozen to −40°C within a Virtis freeze dryer. These solutions did not have crosslinker added.

Both HA solutions produced foams, which were open celled and showed interconnectivity, which appear ideal for cell proliferation, ingrowth, and vascularization. The pore distribution and size were also similar as shown in Figure 2; however, samples produced from 1% solutions had low density and were brittle. Foams prepared from 4% solutions were not as brittle and held their shape, and, for this reason, it was decided to use 4% solutions for further analysis.

Influence of freezing temperature and freezing rate on porosity

HA solutions were frozen on a precooled stainless steel pan at −40°C for 60 min, and the cooling rate was 3.4°C/min. The frozen suspension was then sublimated under a vacuum (of <100 mTorr) overnight. For samples frozen at 0.6°C/min, the shelf was not pre cooled hence the slower rate of cooling. In Figure 3, the average freezing rates of the solutions (0.6°C/min for curves a, b, c and 3.4°C/min for d) were determined by measuring the cooling time from the starting temperature of the solution to a temperature limit of between 2 and 4°C greater than the final temperature of freezing. Below that temperature, the cooling rate of the HA solution tended to slowly and asymptotically approach the final temperature of freezing.

Figure 3 illustrates the temperature profile of the HA solution during freezing, curve (a) frozen to −20°C, (b) frozen to −30°C, (c) frozen to −40°C, and (d) frozen to −40°C. The time required for the liquid–solid transition of the HA solution at the freezing point was ~ 14 min for 0.6°C/min and 2 min for 3.4°C/min. The cellular structure of scaffolds produced using this technique (0.6°C/min) appeared homogeneous throughout the entire scaffold. O'Brien[39,40] found pores produced by a similar

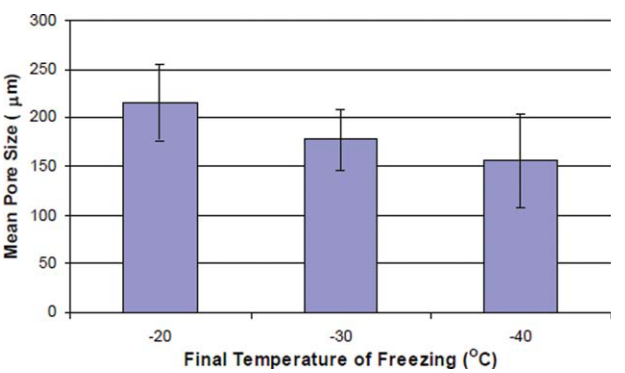

Figure 6 Effect of freezing temperature on the average pore size of foams frozen at ~ 0.6°C/min. Five samples were analyzed at each temperature. [Color figure can be viewed in the online issue, which is available at wileyonlinelibrary.com.]

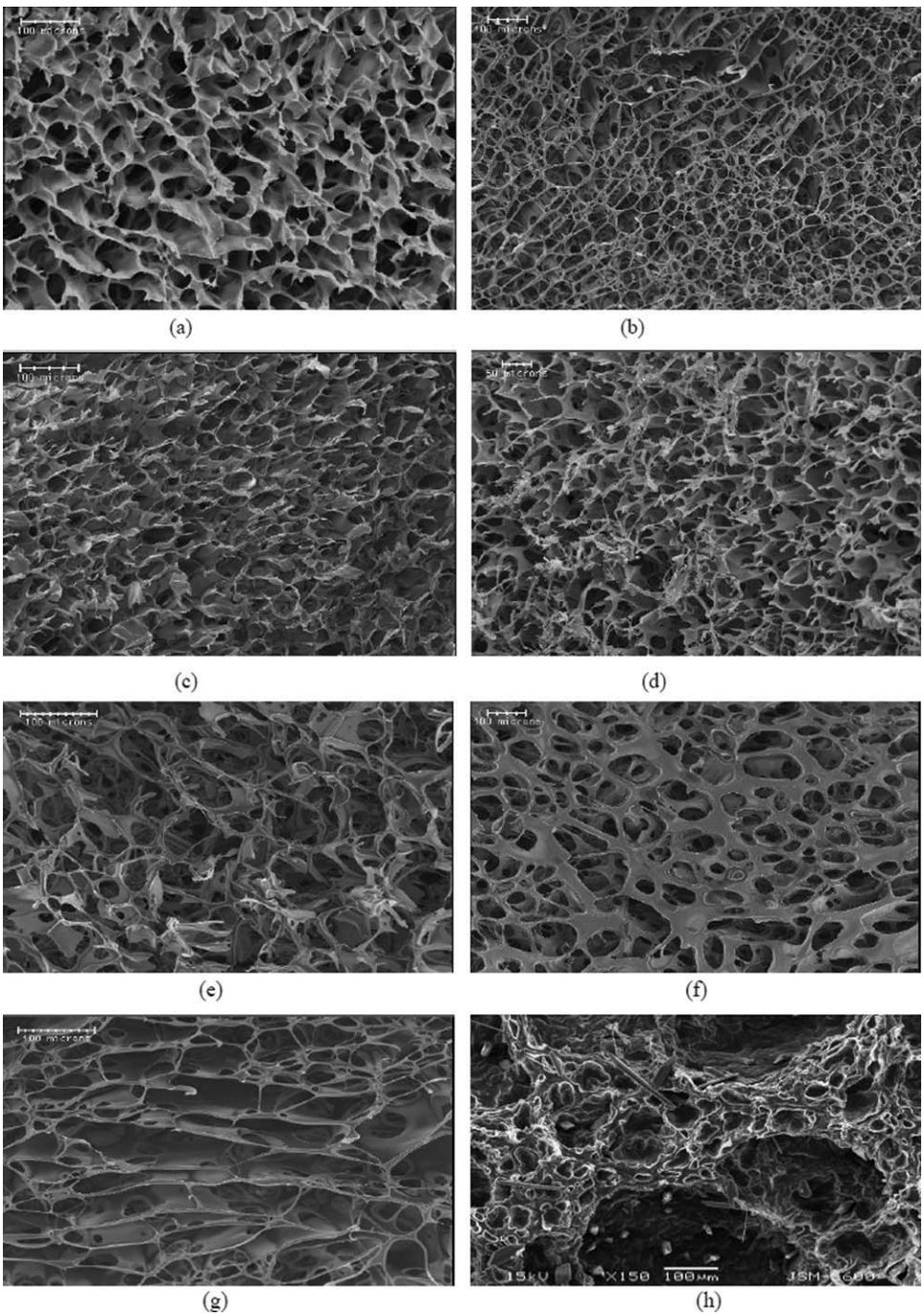

Figure 7 Crosslinked interconnected porous scaffolds (a) immersion crosslinked by DVS (150× magnification); (b) immersion crosslinked by EDC + LME (100× magnification); (c) immersion crosslinked by EX 810(150× magnification); (d) immersion crosslinked by GTA (200× magnification); (e) solution crosslinked by EX810 (200× magnification); (f) solution crosslinked by GTA (100× magnification); (g) solution crosslinked by EDC + LME (200× magnification); and (h) solution crosslinked by DVS (150× magnification).

method were more uniform in size, have a consistent pore structure, and show no obvious variation in mean pore size, pore structure, or alignment throughout the scaffold, when compared with pores produced by a faster freezing rate. This was also the case with these materials, but it was also noticed that the pore structure of the scaffold produced by the fast freezing rate (3.4°C/min) seems to have thin planes of HA that possess tiny pores as shown in Figure 4.

Figure 5 assesses the effect of freezing temperature on the pore size of uncrosslinked materials. These materials were subsequently crosslinked by the immersion method. Sections were taken from the

TABLE I
Physical Properties of Preimmersion Crosslinked Scaffolds and Scaffolds Produced by Solution Crosslinking

Sample	Freezing temperature (°C)	Density (g/cm^3)	Wall thickness (μm)	Average pore size (μm)
Uncrosslinked	−40	8.6×10^{-2}	5	156
Uncrosslinked	−30	7.8×10^{-2}	8	177
Uncrosslinked	−20	8.2×10^{-2}	7	215
DVS	−20	17.6×10^{-2}	60	215
EDC	−20	10.4×10^{-2}	22	170
EX 810	−20	10.2×10^{-2}	34	149
GTA	−20	14.7×10^{-2}	26	167

transverse plane and from the cross section of scaffolds frozen at −10°C and −20°C. Scaffolds produced at a freezing temperature of −20°C showed no significant variation in mean pore size between the transverse and cross sections indicating that the pores formed in these scaffolds were uniform in shape as well as in size, that is, an equiaxed pore structure was produced. However, scaffolds produced at a freezing temperature of −10°C were found to have a significant variation in mean pore size between the transverse and cross sections, suggesting that, at this higher freezing temperature, columnar ice crystals are formed rather than the more equiaxed ice crystals that form at the lower temperatures of freezing as shown in Figure 5. Scaffolds frozen at −30°C and −40°C also produced equiaxed pores.

The average pore diameters of HA solutions frozen at ~ 0.6°C/min to −20°C (215 μm), −30°C (177 μm), and −40°C (156 μm) are shown in Figure 6. A minimum pore size of 150 μm has been suggested in the literature for bone and 200–250 μm for soft tissue,[41–43] and these results show attainment of these target dimensions.

Analysis of pore architecture of crosslinked scaffolds

As a result of the findings above (mechanically stable, possessed appropriate pore distribution, and size), 4% solutions of HA were subject to further development and investigation. The crosslinking solutions gels were then frozen to −20°C and freeze dried to produce the

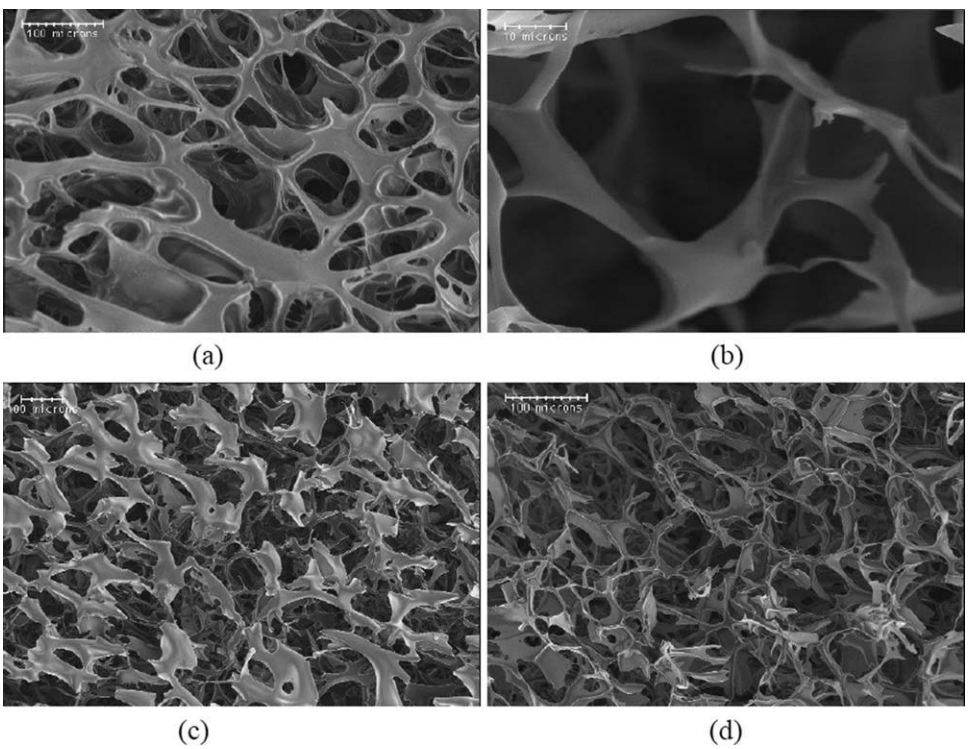

Figure 8 Homogenous hydrogel matrices (a) solution crosslinked scaffold by GTA (200× magnification), (b) solution crosslinked scaffold by GTA (1500× magnification), (c) HA EDC/LME crosslinked scaffold (100× magnification), and (d) HA EDC/LME crosslinked scaffold (200× magnification).

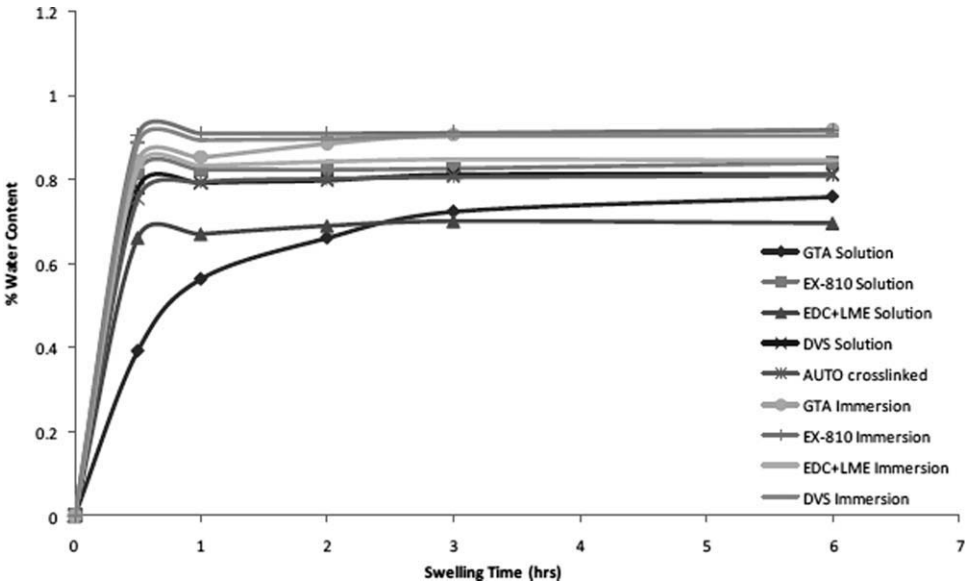

Figure 9 Equilibrium water content of sponges incubated in PBS. Sponges were crosslinked by both the immersion and solution methods.

porous scaffold. After immersion, the sponges were lyophilized by freeze drying. All sponges were kept in a desiccator over silica gel crystals.

The purpose of the crosslinking is to control the mechanical and degradation properties[34,35] of the scaffolds. On comparing the average densities of the crosslinked and uncrosslinked scaffolds, it is apparent from Figure 7 and Table I that the solution crosslinking chemical modification increases the density and wall thickness while decreasing pore size. The data for uncrosslinked samples in Table I represents scaffolds, which were subsequently immersed in crosslinking solution; this method of chemical modification did not have an influence on the scaffold density and wall thickness. However, because the immersion crosslinking method is based on a diffusion mechanism, it can be postulated that thinner walled scaffolds will have higher crosslink densities. Scaffolds crosslinked by the heterogeneous immersion method (a–d) and by the solution method (e–h) are shown in Figure 7. Every effort was made to keep the magnifications consistent however to get the required quality and to avoid charging in the samples some variation was required. Scale bars have been inserted for comparisons.

Some of the pore sizes quoted here are less than the 200–250 μm for soft tissue replacement, but this is not envisaged as a problem as pore enlargement through swelling will occur in an *in vivo* hydrating environment.

The morphology of the homogeneous hydrogel matrices can be described as randomly oriented pores that are interconnected with smaller pores resembling meshes of gel as shown in Figure 8.

Equilibrium swelling studies

Samples were swollen in PBS for 24 h and, and the EWC and sol fractions were evaluated. All the crosslinked HA scaffolds had reached their equilibrium

TABLE II
Characterization of Crosslinked Scaffolds Following Incubation in PBS (n = 5)

	W_d (mg)	W_s (mg)	Wd_1 (mg)	Sol fraction[a]	Swelling ratio	% water
Immersion crosslinked						
DVS	20.3	218.0	19.4	0.04	10.74	90.7
EDC + LME	28.3	186.7	27.9	0.01	6.60	84.8
EX 810	33.4	420.8	32.1	0.04	12.6	92.1
GTA	27.2	341.9	26.0	0.04	12.57	92.0
Solution crosslinked						
DVS	23.3	125.8	22.4	0.04	5.4	81.4
EDC + LME	28.2	87.4	27.4	0.03	3.1	67.7
EX 810	24.6	154.5	23.1	0.06	6.28	84.1
GTA	25.7	107.4	25.2	0.02	4.18	76.1

[a] Sol fraction = 1 – Wd_1/Wd.

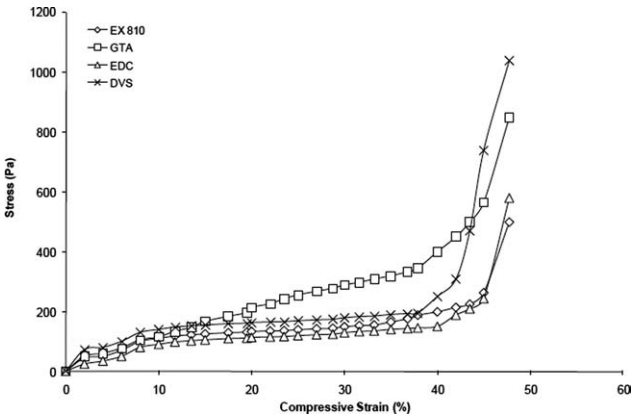

Figure 10 Stress versus compressive strain for hyaluronic acid scaffolds after equilibrium swelling.

swelling at 3 h (Fig. 9). All samples were crosslinked by a HA crosslinker mole ratio of 1 : 2, which yielded good crosslink densities and mechanically stable scaffolds.

The SRs given in Table II indicated the degree of crosslinking attained by a sample. The EDC + LME sample had the lowest SR indicating that this sample had the highest crosslink density. The percentage water was calculated for each sample. The amount of water within the sample is dependant on the amount of crosslinking, and Figure 9 shows the percentage water content as a function of time for all the samples crosslinked by both the immersion and solution techniques. The percentage water content gives an indication of the mechanical integrity of the scaffolds, the lower the water content, the better the mechanical properties, unless the low water content is a result of hydrolytic degradation. The sol fraction is a measure of the amount of uncrosslinked polymer that can be extracted from the scaffold and can be an indication of the effectiveness of the crosslinking procedure. The results suggest that there is a small loss of HA from the scaffold with a maximum of 6%.

Mechanical analysis of porous scaffolds

Figure 10 shows that when subjected to a compressive load, the scaffolds crosslinked by the solution method exhibit two responses; an initial weak response followed by a rapid increase in modulus. This behavior is attributed to the porosity of the samples. As these materials compress, the macropores collapse that allow for large deformation with little stress. When these macropores are mostly closed, the bulk material starts to compress, which results in a higher modulus. For the 60 and 70 vol % samples, these two compression pathways appear to occur in tandem resulting in a stress–strain response between these two extremes.[44] The data in Figure 10 seems to fit this description; therefore, the porosity of the samples can be estimated to be 60–70 vol %.

The overall J curve shape, with a low-initial resistance to deformation, followed by much greater relative stiffness at larger deformation, is similar to that given by body soft tissue. The magnitude of the mechanical response is similar to that of hydrogel scaffolds synthesized from Chitosan.[45] The compression data were only included for solution crosslinked scaffolds as the immersion crosslinked samples were too brittle to sustain the compression load.

CONCLUSIONS

The ideal combination of material formulation and combination of freeze drying conditions for the production of porous HA scaffolds, displaying interconnectivity and a pore size suitable for a soft tissue scaffold were found to be a 4% w/v HA solutions frozen to −20°C at a rate of 0.6°C/min solution crosslinked with EDC plus LME. In general, the solution-crosslinking method produced scaffolds with higher crosslink densities, lower SRs, and improved mechanical performance. The literature[23–26] confirms that HA-based materials are both biocompatible and bioresorbable. It is recognized that some of the reagents used for crosslinking are cytotoxic, and it will be important to establish that there is no residual crosslinker present in the final cellular products.

A minimum pore size of 200–250 μm for soft tissue scaffolds has been suggested in the literature[43–46] as optimum and the scaffolds fabricated here have a pore size within the 200–250 μm range and are therefore expected to encourage tissue ingrowth. The scaffolds showed sufficient mechanical integrity to support cell attachment and growth and could provide the newly regenerating tissue with a temporary site for cell attachment and proliferation.

References

1. Bell, E. Tissue Eng 1995, 1, 163.
2. Naughton, G.; Tolbert, W.; Grillot, T. Tissue Eng 1995, 1, 211.
3. Drury, J. L.; Mooney, D. J. Biomaterials 2003, 24, 4337.
4. Atala, A.; Lanza, R. P. Methods of Tissue Engineering; Academic Press: USA, 2002.
5. Chen, G.; Ushida, T.; Tateishi, T. Mater Sci Eng C 2001, 17, 63.
6. Griffith, L. G. Acta Mater 2000, 48, 263.
7. Chen, G. P.; Ushida, T.; Tateishi, T. Macromol Biosci 2002, 2, 67.
8. Chaignaud, B. E.; Langer, R.; Vacanti, J. P. In Synthetic Biodegradable Polymer Scaffolds, Vol.1;Atala, A., Ed.; Birkhauser: Boston, 1987.
9. Park, J.; Lakes, R. Biomaterials: An Introduction. New York: Plenum Press, 1992.
10. Ratner, B. D.; Hoffmann, A. S.; Schoen, F. J.; Lemons, J. E. Biomaterials Science: An introduction to Materials in Medicine. San Diego, CA: Academic Press, 1996.
11. Shoichet, M. S.; Hubbell, J. A. Polymers for Tissue Engineering. Utrecht: Ridderprint bv, 1998.

12. Silver, F. H.; Christainsen, D. L. Biomaterials Science and Biocompatibility. New York: Springer, 1999.
13. Williams, D. Fundamental Aspects of Biocompatibility. Boca Raton, FL: CRC Press, 1981.
14. Park, S. N.; Lee, H. J.; Lee, K. H.; Suh, H. Biomaterials 2003, 24, 1631.
15. Bent, A.; Foote, J.; Siegel, S.; Faerber, G.; Chao, R.; Gormley, E. J Urol 2001, 166, 1354.
16. Loebsack, A.; Greene, K.; Wyatt, S.; Culberson, C.; Austin, C.; Beiler, R. J Biomed Mater Res 2001, 57, 575.
17. Lee, K.; Rowley, J.; Eiselt, P.; Moy, E.; Bouhadir, K.; Mooney, D. Macromolecules 2000, 33, 4291.
18. Tabata, Y.; Miyao, M.; Ozeki, M.; Ikada, Y. J Biomater Sci: Polym Ed 2000, 11, 915.
19. Okano, T.; Matsuda, T.; Mosahebi, A. Cell Transpl 1998, 1, 71.
20. Mao, J. S.; Liu, H. F.; Yin, Y. J.; Yao, K. D. Biomaterials 2003, 24, 1621.
21. Mann, B.; Schmedlen, R.; West, J. Biomaterials 2001, 22, 439.
22. Hutmacher, D. J Biomat Sci Polym 2001, E12, 107.
23. Turley, E. The science of hyaluronan today 1999 [cited 2007 July 15]; Available from: http://www.glycoforum.gr.jp/index.html.
24. Hardingham, T. Sci Hyaluronan Today 1998 [cited 2007 July 15]; Available from: http://www.glycoforum.gr.jp/index.html.
25. Knudson, W.; Chow, G.; Knudson, C. B. Matrix Biol 2002, 21, 15.
26. Knudson, W.Knudson, C. Sci Hyaluronan Today 1999 [cited 2007 July 15]; Available from: http://www.glycoforum.gr.jp/index.html.
27. Laurent, C.; Hellstrom, S.; Stenfors, L. Am J Otolaryngol 1986, 7, 181.
28. Fukuda, K.; Takayama, M.; Ueno, M.; Oh, M.; Asada, S.; Kumano, F. Inflamm Res 1997, 46, 114.
29. Balazs, E. In A guide to its use in ophthalmic surgery, Vol. 5; Miller D, Stegmann R, Eds.; Wiley: New York; 1983.
30. Balazs, E. A.; Denlinger, J. L. Ciba Foundation Symp 1989, 143, 265.
31. Avitabile, T.; Marano, F.; Castiglione, F.; Bucolo, C.; Cro, M.; Ambrosio, L. Biomaterials 2001, 22, 195.
32. Yeo, Y.; Highley, C. B.; Bellas, E.; Ito, T.; Marini, R.; Langer, R. Biomaterials 2006, 27, 4698.
33. Ito, T.; Yeo, Y.; Highley, C. B.; Bellas, E.; Benitez, C. A.; Kohane, D. S. Biomaterials 2007, 28, 975.
34. Collins, M. N.; Birkinshaw, C. J Appl Polym Sci 2007, 104, 3181.
35. Collins, M. N.; Birkinshaw, C. J Appl Polym Sci 2008, 109, 923.
36. Collins, M. N.; Birkinshaw, C. J Mater Sci: Mater Med 2008, 19, 3335.
37. Yahia, L. Ligaments and Ligamentoplasties. Berlin: Springer-Verlag, 1997.
38. Tienen, T.; Heijkants, R.; Buma, P.; Groot, J.; Pennings, A.; Veth, R. Biomaterials 2002, 23, 1731.
39. Tokita, Y.; Okamoto, A. Polym Degrad Stab 2002, 48, 269.
40. O'Brien, F.; Harley, B.; Ioannis, Y.; Gibson, L. Biomaterials 2004, 25, 1077.
41. O'Brien, F.; Harley, B.; Yannas, I.; Gibson, L. Biomaterials 2005, 26, 433.
42. Spector, M.; Michno, M.; Smarook, W.; Kwiatkowski, G. J. Biomed Mater Res 1978, 12, 45.
43. Cooper, J. A. Design, Optimization and In Vivo Evaluation of a Tissue-Engineered Anterior Cruciate Ligament Replacement. Drexel University: Philadelphia, USA, 2002.
44. Von-Recum, A. F. Handbook of Biomaterials Evaluation: Scientific, Technical and Clinical Testing of Implant Materials; Macmillan: New York, 1986.
45. Dziubla, T. D. Macroporous Hydrogels as Vascularizable Soft Tissue—Implant Interfaces: Materials Characterization, In Vitro Evaluation, Computer Simulations, and Applications in Implantable Drug Delivery Devices. Drexel University: Philadelphia, USA, 2002.
46. Nettles, D. L. Evaluation of Chitosan as a Cell Scaffolding Material for Cartilage Tissue Engineering. Mississippi State University: Mississippi, USA, 2001.